Liquid Structure of a Choline Chloride-Water Natural Deep Eutectic Solvent: a Molecular Dynamics characterization.

Alessandro Triolo[1,*], Fabrizio Lo Celso[1,2], Martin Brehm[3], Valerio Di Lisio[4] and Olga Russina[1,4,*].

[1] Laboratorio Liquidi Ionici, Istituto Struttura della Materia, Consiglio Nazionale delle Ricerche, (ISM-CNR) Rome, Italy

[2] Department of Physics and Chemistry, Università di Palermo, Palermo, Italy.

[3] Institut für Chemie, Martin-Luther-Universität Halle–Wittenberg, Halle (Saale), Germany.

[4] Department of Chemistry, University of Rome Sapienza, Rome, Italy.

Corresponding Authors: A. T. (triolo@ism.cnr.it); O.R. (olga.russina@uniroma1.it)

Abstract.

The liquid structure of a representative of the first water-in-salt (WiS) Natural Deep Eutectic Solvents (NADES), hereinafter indicated as *aquoline*, a mixture of choline chloride (ChCl) and water with molar ratio 1:3.33, is explored at ambient conditions. Using Molecular Dynamics (MD) simulation tools, we extract structural information at atomistic level on the nature of inter-correlations between the different moieties. Despite being a very fluid liquid, with much lower viscosity than other common ChCl-based DES, aquoline turns out to be very structured. Computed X-ray and neutron weighted scattering patterns (the latter also on selectively deuterated mixtures) highlight the existence of mesoscopic organization that is rationalised in terms of choline vs. water/chloride structural alternation. The study shows that choline cations are highly coordinating the surrounding environment: strong hydrogen bonding mediated correlations between the hydroxyl group and water or chloride are detected. In addition, the ammonium group drives the formation of a complex solvating environment, with water, chloride and hydroxyl moieties approaching it, between the hindering methyl groups. Strong hydrogen-bonding interactions between water molecules and between water and anions are detected and, while water cannot create a bulk water-like environment around itself, its network with neighbour water or anions develops long chains across the bulk phase. This is a first study that will be extended based on complementary experimental work as a function of water content and temperature/pressure, to explore structural and dynamic properties of this class of materials.

Introduction.

Choline (Ch, 2-hydroxyethyl-trimethylammonium, vitamin B4) chloride (ChCl) is a nutritional additive and often added as a supplement to animal food. It is a safe, non-toxic, biodegradable and easily accessible ionic compound. It is one of the most well-known components of natural deep eutectic solvents (NADES), which is a subset of Deep Eutectic Solvents (DES). [1–5] (NA)-DES are presently attracting great attention as an environmentally sustainable class of materials addressing several societal calls. DES are a class of compounds prepared as binary mixtures of two components, with DES's freezing point being largely below the melting points of the two components. DES are typically prepared by mixing ionic compounds, such as ChCl, with hydrogen bonding (HB) donor (HBD) compounds.[6–11] One of the most well-known DES is a stoichiometric mixture of ChCl and urea at molar ratio 1:2 (often indicated as Reline), with urea behaving as the HBD agent.[6,8,9,11] Other common DESs involve glycerol[12] (leading to glyceline), ethylene glycol[7] (leading to ethaline) or sugars[13] as HBDs at given stoichiometric ratios. DES' structure has been explored in details in the last few years and the synergy between X-ray/neutron scattering and computational tools allowed extracting fundamental knowledge on the nanoscopic organization in these appealing media.[11,14–17] Reline is among the most studied DES, from this point of view. Neutron scattering studies have been conducted on this DES and the corresponding computational modelling allowed describing its structural features, as due to an intricate blending of large to medium strength HB interactions, leading to a sandwich structure, where chloride anions are wrapped by HB interacting cations and urea, in a locally stoichiometrically determined fashion.[11,18] Related computational studies[17] showed the important role played by urea in interacting through HBs with both Ch and Cl in reline: this was not observed for the HBD in other common DES such as glyceline and ethaline, where a preference for intra-HBD interactions is found instead, leading to weaker Cl intercalation. Such differences were related to different acidities of the amide and hydroxyl functional groups in the HBD. Moreover, the fact that glycerol and ethylene glycol are more flexible than urea plays a weakening effect on the hydrogen bond network. In this scenario, the presence of water has often been considered as potentially detrimental, although the consistent decreasing of viscosity upon water addition can positively influence DES properties. Edler and coworkers showed how water addition can influence the structure of reline,[16] and the structure of reline-water mixtures have been studied also by other groups, e.g. reff.[19,20]. The structural effect of water on DES has been studied in malicine (ChCl-malic acid 1:1), as well.[15] In these studies, the water content has been found to be important in affecting structural properties and even structural homogeneity in DES. Limited water additions are not efficient enough to affect the resilient DES structural organization, which maintains mostly unaltered; however at larger water contents (e.g. 83

mol-% in reline) substantial changes are observed in the DES components' surroundings and the system needs to be considered as an aqueous solution of DES components, rather than a DES.[16]

Recently the HBD capability of water has been taken into consideration to attempt the formation of a NADES, composed solely by ChCl and water, the latter playing the role of the HBD component, rather than behaving as a contaminant or an additive.[21] Upon ChCl mixing with water, mixtures with ChCl/H_2O molar ratio in the range between 1 : 3.3-4.2, showed no sign of crystallization, upon cooling. On the basis of their Brillouin characterization, Gutierrez and coworkers estimated the eutectic composition for such a system at ChCl/H_2O molar ratio 1:4.2; for such mixtures they provided density and viscosity data at 25 °C.[21] During the revision of the manuscript, we also got aware of a paper dealing with the preparation and characterization of two related systems, namely: ChCl/H_2O with molar ratio 1:3 and 1:4.[22]

More in perspective, the proposed mixtures are framed into the recently proposed scenario of aqueous salt hydrates that are suggested as *unconventional* DES (*u*DES) [23]. Such a kind of DES is prepared by mixing water and congruently melting salt hydrates[23] (in the present case the lower hydrate ChCl$(H_2O)_2$). In this context, we mention that the peculiar chemical composition of these compounds (binary mixtures of salt and water) makes them fit into the group of water-in-salt (WIS) systems that is presently attracting a great deal of attention for electrochemical applications.[24–27] We stress then that the presently investigated compound belongs to both the *u*DES and WIS categories, thus representing a very interesting system to explore.

In this contribution, we aim at providing the first structural characterization of a binary mixture of ChCl with water at molar ratio 1:3.33, a composition in the eutectic range as reported in ref. [21]. Hereinafter, for the sake of clarity we identify this compound as *aquoline*, a term to be used to refer to such a system and, in principle, to the eutectic compound, whenever its composition will be identified in a more accurate way. Aquoline (see Scheme 1) is a quite concentrated mixture of salt and water, with ChCl amounting to 70 wt.-% and, despite its low viscosity ($\eta_{25°C}$=12.23 cP, $\eta_{25°C}$ for Reline is 1400 cP[28] or $\eta_{35°C}$ for ethaline is 30 cP[29]), a strong, HB-mediated, interacting network is expected to take place between the different moieties in this mixture.

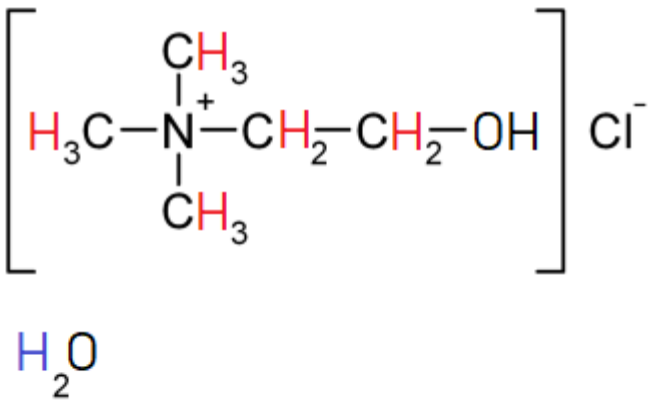

Scheme 1. Schematic representation of Aquoline components, Choline Chloride and water. Red and blue coloured symbols, in choline and water, respectively, refer to the hydrogen atoms that have been selectively replaced with deuterium, in order to change neutron contrast.

ChCl is well known to form two lower hydrates, a stable di-hydrate and an unstable mono-hydrate.[30] The former compound, $ChCl\cdot(H_2O)_2$, melts at 9 °C and can be easily prepared from the anhydrous salt. It is well-known that quaternary ammonium salts are very efficient in driving strong water structuration around themselves when in aqueous solution.[30,31] In the case of the liquid di-hydrate, Harmon et al. observed that water molecules lead to IR spectra strongly resembling those of other analogous hydrates that are crystalline at ambient conditions (e.g. tetramethylammonium hydroxide pentahydrate).[30] The same liquid di-hydrate was studied by ^{1}H-NMR and it appears that proton exchange between choline hydroxyl and water is either very slow or not occurring. These evidences led the authors to propose a structural model where choline hydroxyl group forms strong O–H··Cl hydrogen bonds, while the chloride ions are embedded into a framework clathrate by surrounding water molecules.[30]

Dilute aqueous solutions of ChCl have been studied from the structural standpoint in the past. The Maginn group reported molecular dynamics simulations on the liquid structure of two aqueous mixtures of ChCl at two different conditions.[32] The probed concentrations are much more dilute than the ones probed herein and the authors find that both ions are fully solvated by water. More recently, Buchner and coworkers probed hydration and ion association in ChCl dissolved in water, by means of experimental tools (dielectric spectroscopy and conductivity) and computational

methods probing ChCl in water at infinite dilution.[33] To our knowledge, no structural information is available on concentrated mixtures of ChCl with water in the composition range relevant for the NADES formation. Recently ChCl aqueous solutions have been studied by Vilas-Boas et al., who reported solubility and density data for a series of salts dissolved in water, including ChCl, in the range between 0.1 and 0.3 molar fraction.[34]

Experimental methods.

ChCl was a TCI-Chemicals product (>99%). Before use, it was kept at 40°C under high vacuum to remove moisture and hence after kept in anhydrous environment. ChCl was weighted inside a glove box with dry atmosphere. MilliQ water was used to prepare aquoline with the previously prepared dried ChCl. The mixture was kept agitated for one hour at ca. 50°C, in order to achieve a homogenous, limpid and transparent liquid. Such a sample was kept in a tight vial before any measurement, to avoid moisture contamination.

DSC thermograms were acquired by a Mettler Toledo DSC 822e equipped with a FRS5 sensor and a liquid nitrogen cooler. The furnace was purged during the measurement with dry nitrogen at a flow rate of 30 ml min^{-1}. A sample of about 5 mg was weighted in a 40 μl aluminium pan and rapidly sealed. DSC scans comprised of a cooling from 20 to -150 °C followed by a heating from -150 °C up to 50 °C, with a heating/cooling rate of 10 °C min^{-1} .

Small Angle X-ray Scattering (SAXS) measurements were performed at the SAXSLab Sapienza with a Xeuss 2.0 Q-Xoom system (Xenocs SA, Sassenage, France), equipped with a micro-focus Genix 3D X-ray source (λ = 0.1542 nm), a two-dimensional Pilatus3 R 300K detector which can be placed at variable distance from the sample. Calibration of the scattering vector Q range, where $Q=(4\pi \sin\theta)/\lambda$, 2θ being the scattering angle, was performed using a silver behenate standard.

Measurements with different sample-detector distances were performed so that the overall explored Q region was $0.1 < Q < 3$ $Å^{-1}$. The sample was loaded into a disposable quartz capillary with nominal thickness 1.0 mm and sealed with hot glue before placing it in the instrument sample chamber at reduced pressure (~0.2 mbar). The beam size was defined through the two-pinhole collimation system equipped with scatterless slits to be 0.25 mm x 0.25 mm.

The two-dimensional scattering patterns were subtracted for the dark counting, and then masked, azimuthally averaged and normalized for transmitted beam intensity, exposure time and subtended solid angle per pixel, by using the FoxTrot software developed at SOLEIL. The one-dimensional S(Q) vs. Q profiles were then subtracted for the capillary contribution.

The measurement was conducted at ambient temperature (ca. 20°C) and the sample maintained liquid and homogeneous during the whole length of the experiment.

Computational methods.

Molecular dynamic simulations were performed using the GROMACS 2018.3 package software.[35,36] Bonded and non bonded parameters for choline chloride were described using an all-atoms OPLS force field developed by the group of Acevedo,[37] while TIP3P potential was used for water.[38]

The simulation for aquoline was performed using a cubic box of 1200 choline chloride pairs and 4000 water molecules, applying periodic boundary conditions. Initial configurations were created by Packmol software,[39] the starting density was fixed about 10% higher than the experimental one. The equilibration procedure was done in several steps, starting from a 2 ns NVT simulation at 400 K, followed by a series of 2 ns NPT runs lowering progressively the temperature from 400 K to 350 K and then to 298 K; pressure was fixed for at 1 bar using a Berendsen barostat [40].

After the equilibration phase, the simulation ran for 50 ns for production, and then the trajectory of the last 20 ns was used for calculation of structural properties. The simulation was constantly monitored for the energy and density profile. During the production run, for the temperature coupling we used a velocity rescaling thermostat[41] (with a time coupling constant of 0.1 ps); for the pressure coupling, we used a Parrinello–Rahman barostat[42] (1 ps for the relaxation constant). The Leapfrog algorithm with a 1 fs time step was used for integrating the equations of motion. Cut-offs for the Lennard- Jones and real space part of the Coulombic interactions were set to 16 Å. For the electrostatic interactions, the Particle Mesh Ewald (PME) summation method[43,44] was used, with an interpolation order of 6 and 0.08 nm of FFT grid spacing. Pair correlation, angular and spatial distribution functions were obtained using the TRAVIS software[45–47].
X-ray and neutron scattering patterns were computed using TRAVIS.[45–47] In the case of neutron-weighted scattering patterns computations, different selectively labelled samples were considered, with either all species hydrogenated, ChCl-H_2O (i.e. no deuteration) (HH mixture), or ChCl-D_2O (HD mixture) or d13ChCl-H_2O (DH mixture) or d13ChCl-D_2O (DD mixture) (see Scheme 1). Scattering patterns decompositions were computed using in house developed codes;[48–51] network analysis for the detection of chain morphology has been developed using ChemNetworks.[52]

Results and Discussion.

Aquoline has been investigated by Zhang et al., who provide density, viscosity, DSC traces and Brillouin data for a range of ChCl-H_2O mixtures, including 1:3.3.[21] A density data set for ChCl molar fraction between 0.1 and 0.301 has also been reported at 25 °C by Vilas-Boas et al.[34] Zhang et al. report a value of 1.08882 g/cc;[21] extrapolation of data reported in ref. [34], leads to a value of 1.09173 g/cc. Our simulation equilibrates at a value of 1.094 g/cc, which overestimates the experimental data by less than 0.5%, thus providing excellent support to the reliability of the chosen force fields used for the MD simulations to account for structural organization in bulk aquoline.

In view of the claims recently reported in [22], we determined the thermal behaviour of our present sample of aquoline. In **Figure S1** of the SI, we report the corresponding thermal trace collected at 10°C/min upon both cooling and heating. It clearly emerges the presence of a glass transition at ca. -130 °C. During the heating scan, the small endothermic overshoot at about -125 °C is ascribed to the enthalpic recovery from the glassy to the liquid state.[53] Crystallization of the sample could be excluded because of the absence of endo- and exothermic features in the liquid region of the thermogram, in agreement with the data from [21]. We propose that the claimed crystallization reported in ref. [22], might be a consequence of the limited temperature range explored during the measurements.

Figure 1 shows MD-derived X-ray and neutron scattering patterns from liquid aquoline. While these data sets remind analogous ones obtained for other DES, here it is noteworthy that a distinct scattering feature emerges at low Q values, especially in neutron patterns (below 1.5 $Å^{-1}$). X-ray scattering data (in the inset) show a main peak centred at 1.8 $Å^{-1}$ with a shoulder at 2.2 $Å^{-1}$ (a Q range where water is known to show a peak), otherwise they are essentially featureless below 1.5 $Å^{-1}$ (however, a weak shoulder can be detected at ca. 1.3 $Å^{-1}$). We report the experimental SAXS pattern from aquoline at 20°C in Figure S2 of the SI and this data set confirms the complex features reported in the inset of Figure 1 in the range below 3 $Å^{-1}$. The case of neutron scattering data sets is much more articulated. The natural mixture (i.e. no selective deuteration is considered, the sample is indicated as HH, where the first letter refers to choline and the second to water) shows a pattern with peaks centred at 1.25 and 1.9 $Å^{-1}$. Upon deuteration of methyl and methylene groups in choline

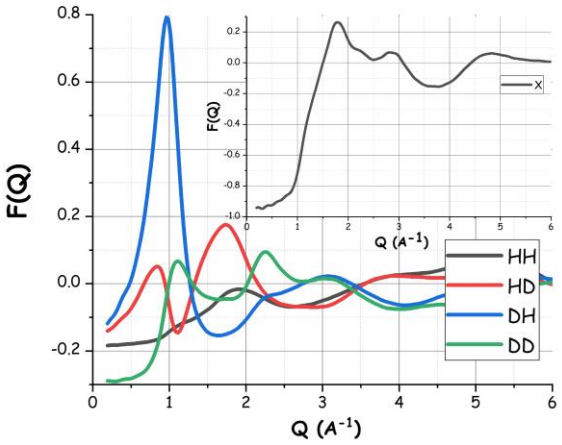

Figure 1. MD derived neutron weighted static structure factors, as obtained from MD simulations of aquoline at 298 K. The different codes for the sample H/D, refer to protium/deuterium substitution in choline or water, respectively. In the inset, the corresponding computed X-ray scattering pattern is shown.

or of water, however, the patterns drastically change, with the development of a strong scattering feature at 1.1, 1.0 and 0.9 $Å^{-1}$ for DD, DH and HD, respectively. Especially in the case of deuterated choline and H_2O (DH mixture), such a peak becomes very intense. Neutron data reported for neat reline by Hammond et al.[11] and Gilmore et al.[8] show such a feature in the case of choline chloride

mixed with deuterated urea (equivalent to our HD mixture, when urea replaces water, as a HBD). Also the neutron scattering data reported by Hammond et al. on reline mixed with water show that when deuterated water is added, a feature similar to the one reported herein shows up,[16] but the authors did not further discuss this issue.

While not many DES have been explored using H/D substitution supported neutron scattering

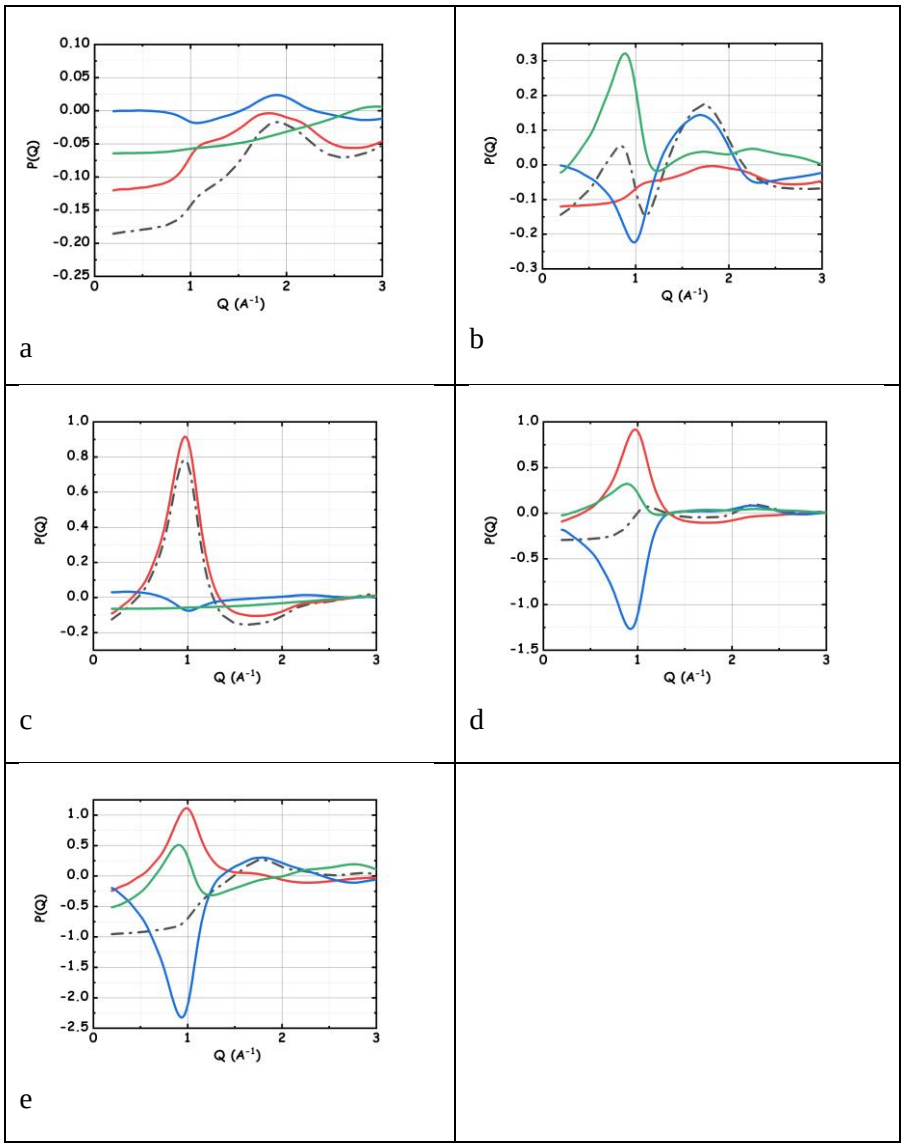

Figure 2. Low Q portions of MD derived neutron (a)-d)) and X-ray (e)) weighted static structure factors, as obtained from MD simulations of aquoline at 298 K. The reported patterns have been decomposed in three contributions arising from: a) self-correlation of water and Cl ([A; A] term, green line); self-correlation of Ch ([B; B] term, red line) and c) cross-correlation of Ch with water and Cl ([A; B] term, blue line). The total term is given by the black dashed line. The four neutron weighted patterns refer to the following deuteration substitutions: [water&Cl; Ch]= a) [H; H], b) [H, D], c) [D, H] and d) [D, D].

experiment, aquoline looks like a prominent example of a DES characterised by the existence of

structural correlations over a distance of several Å. In **Figure 2**, the low Q portions of the scattering patterns of **Figure 1** have been decomposed into three terms, arising from two main components. One is composed by water and chloride together (indicated as moiety A) and the other is composed by choline (indicated as moiety B). We decompose the computed diffraction patterns as the combination of the interaction of each component either with itself or with the other. Accordingly, in **Figure 2**, the decomposition of P(Q) in terms of the two self-terms [A; A] and [B;B] and the cross term [A;B] is shown. Such a decomposition of P(Q) is common in other related fields, when aiming at detecting the alternating components that account for the existence of specific scattering features.[48,50,54–59] Here, although we cannot properly speak about a polar-apolar alternation, which was present in other systems,[48,50,54–56,59] nevertheless we detect that a pseudo-periodic alternation of choline with water/chloride can efficiently account for the existence of the low Q scattering features detected by neutron scattering at ca. 1 $Å^{-1}$. In particular we find that the blue curve corresponding to the cross term [A;B] shows a deep minimum at ca. 1 $Å^{-1}$ out of phase with a maximum of the self terms ([A; A] and [B;B], red and green curves, respectively). Such a behaviour is characteristic of pseudo-alternating domains of A and B species in the liquid structure (see e.g. reffs. [48,50,54,60,61]).

Further insight into atomistic correlations in liquid aquoline will now be obtained using different tools: the main one being radial pair distribution function (PDF) (also known as radial distribution function and indicated as g(r)) that accounts for the normalised probability of distribution of atomic species j at a given, isotropically averaged, distance r from a reference species i, $g_{ij}(r)$. We will also derive the average coordination numbers (CN) by integrating the corresponding PDFs over a distance covering the first minimum beyond the PDF peak. In **Figures 3-5** also running CNs are reported as dashed lines. In **Figure 3**, we show the PDFs (continuous lines) referring to mutual correlations of centers of mass (CoM) of the three different species in aquoline (Ch, Cl and H_2O (w)). The corresponding plots referring to other DES such as ChCl:Urea (1:2, Reline),[8,11] ChCl:oxalic acid (1:1, oxaline),[14] ChCl: Malic acid (1:1, malicine),[62] ChCl:ethylene glycol (1:2, ethaline),[58] show several analogies in the organization of

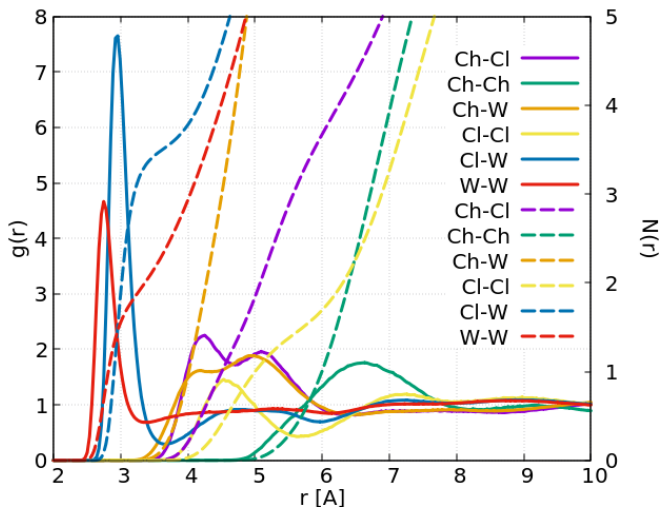

Figure 3. Pair distribution functions (continuous lines, left axis) and coordination number (dashed lines, right axis) of the centers of mass of choline (Ch), chloride (Cl) and water (W), as obtained from MD simulations of aquoline at 298 K.

different species in ChCl-based DES. Nevertheless, a peculiarity of the present system is the fact that the spatial extent of inter-CoM correlations in aquoline falls into three different regimes. It clearly emerges from the inspection of **Figure 3**, that correlations water-water and water-chloride are characterised by short sizes for the first solvation shell that is fingerprinted by the first peak: W-W and W-Cl have a first peak at distances < 3.5 Å. At the other extreme of spatial extent, i.e. r>6 Å, the correlation between Ch-Ch is detected. Finally at intermediate spatial scale, between 3.5 and 6 Å, one finds those CoM-CoM correlations between choline and water / chlorine as well as Cl-Cl. This strong separation in the spatial extent of CoM correlations is due to the large difference in size of both water and chloride from choline, as well as to the coulombic interaction between likely charged ions (Cl-Cl and Ch-Ch).

Ionic species PDF's resemble those found in the other DES: Ch-Ch PDF shows a peak at 6.5 Å (corresponding to a number of nearest neighbours of ca. 8, similarly to reline (6.7)[11]); Ch-Cl PDF shows a splitted first peak with peaks centred at 4.2 and 5.1 Å, with ca. 4 chlorides surrounding reference choline in the first shell (r<6 Å). The latter behaviour resembles the one found in reline at ambient temperature[11], where the two environments correspond to a chlorine distribution around the choline hydroxyl group (at shorter distances, ca. 1.3 neighbours) and another around the ammonium group at larger distances, with ca. 2.7 neighbours.

Choline-water PDF (**Figure 3**) is characterised by a double peak feature at 4.1 and 5.0 Å with ca. 12 water molecules surrounding the reference choline cation. Such a bimodal distribution is similar to the one proposed for chlorine solvation, with two preferred locations as water can distribute either around the hydroxyl or around the ammonium moieties.

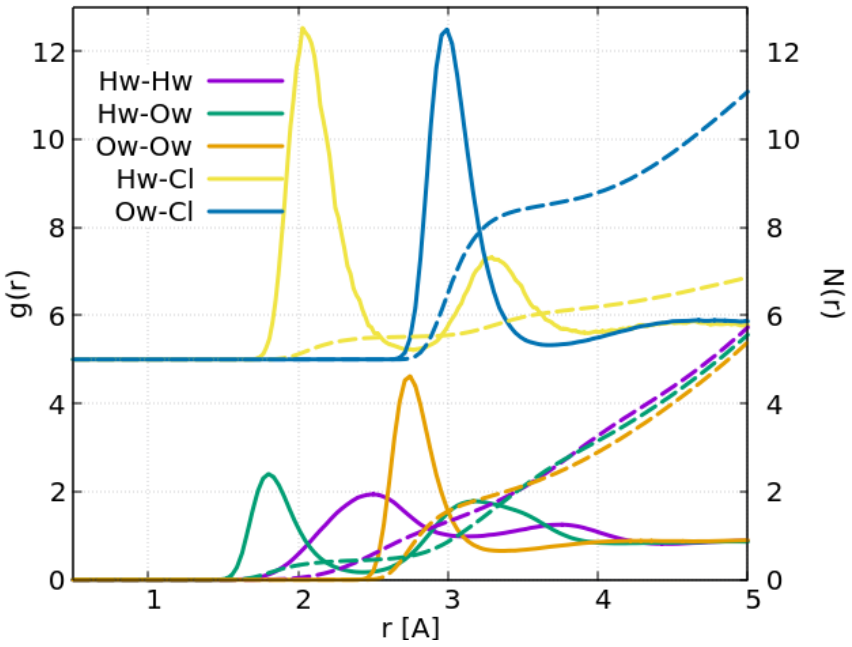

Figure 4. Pair distribution functions (continuous lines) and coordination number (dashed lines, same colour code as for pdfs) referring to water components (Hw and Ow) and chlorine anion, as obtained from MD simulations of aquoline at 298 K. Curves referring to chlorine correlations have been vertically shifted (+5).

Water-water and water-chloride PDFs show the strongest features in this plot and have first peaks at 2.8 and 3.0 Å, respectively. Such interactions are better described by inspection of **Figure 4**, where PDFs related to water components (Ow and Hw) and chloride are shown in detail. On average, each chloride is surrounded by 3.5 water molecules, while each water molecule is surrounded by ca. 2 neighbour water molecules (while, in neat water, this amounts to ca. 4.7 [63]) and ca. one chloride anion. Beyond the first Ow-Ow solvation shell (i.e. above 3.5 Å), the PDF is characterised by amplitude maintaining sensibly below unity, highlighting the existence of a water –water depletion region. This was not the case for other DES, where the HBD-HBD PDFs showed well defined first and second solvation shells (see e.g. ref. [11] for reline, ref. [58] for ethaline, ref. [8] for oxaline). Due to its small size and to the strong interactions with both chloride and choline (vide infra), water cannot organise with surrounding water molecules in an environment resembling that in bulk water.

Overall we observe that chloride can efficiently interact with both water and choline, similarly water can be found efficiently solvating both types of ions.

In the case of Ch, one can expect a complex distribution of neighbour molecules, considering the presence of the charged ammonium nitrogen, the hydrophobic methyl groups and the hydroxyl moiety. In this system, we find that the same behaviour reported in reline applies: the structure is dictated by a complex intertwining of different moieties rather than by the intercalation of water into an onion-like ionic organization.[11] Accordingly, in **Figure 5**, we report selected PDFs referring to the distribution of different moieties around either the oxygen (Och) or the nitrogen (Nch) in choline. A straightforward inspection of these figures shows that coordination around the oxygen atoms is better organised that in the case of nitrogen, the solvation peaks being much closer to the reference atom and narrower in the first case than in the second. This presumably depends on the fact that oxygen is not sterically hindered by the methyl groups that surround nitrogen, thus allowing close and direct contacts. It can be noticed that water oxygen approaches Och closer (by ca. 0.2 Å) than the anion, this behaviour is similar to the one reported for hydrated reline.[64] However, at odd with the behaviour observed in reline,[64] in aquoline, it is the HBD (water), and not the anion, that succeeds to more efficiently solvate the hydroxyl group: we estimate 0.7 surrounding water molecules vs. 0.4 chlorides in the first solvation shell. Accordingly, in aquoline, the choline hydroxyl group prefers to hydrogen bond with water rather than with the chloride anion. We will further explore this point related to the nature of water vs. chloride interaction with the choline's hydroxyl group.

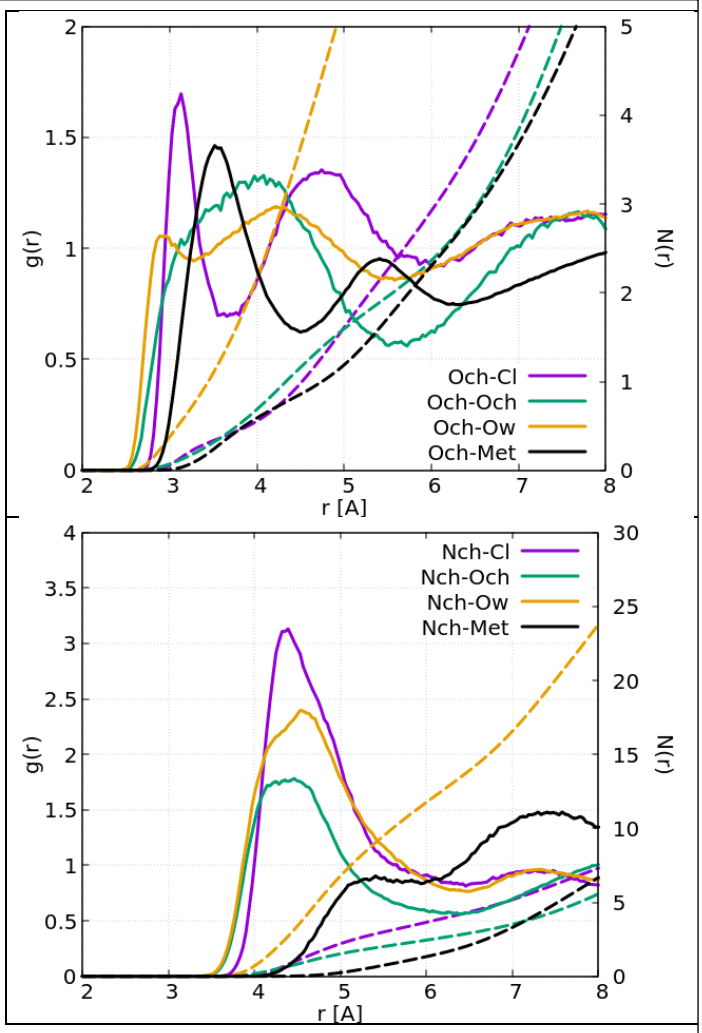

Figure 5. Pair distribution functions (continuous lines, left axis) and coordination number (dashed lines, same colour code as pdf, right axis) referring to the coordination of Choline's oxygen (top) and nitrogen (bottom) by different species, as obtained from MD simulations of aquoline at 298 K.

Analogously, we find that choline's nitrogen solvation (**Figure 5 bottom**) is also due to a competition between the anion and water: one can notice highly structured solvation shells between 3.5 and 6 Å, where also the choline hydroxyl group efficiently penetrates. However, the first solvation shell is predominantly occupied by water molecules (up to 14) and only ca. 5 anions can be detected, together with 3 hydroxyl groups.

Overall, water succeeds to efficiently solvate both polar heads of choline: this makes sense, considering the nature of the hydroxyl group and the known ability of water to strongly solvate alkylammonium moieties.[30,31]

Finally, cation-cation interaction, involving Och and Nch, though hindered by the methyl groups presence, leads to up to 3 Nch's surrounding the hydroxyl group.

The spatial distribution functions (SDF) of different moieties around a reference choline can help in better understanding the so far discussed solvation features. In **Figure 6**, the distributions of anions

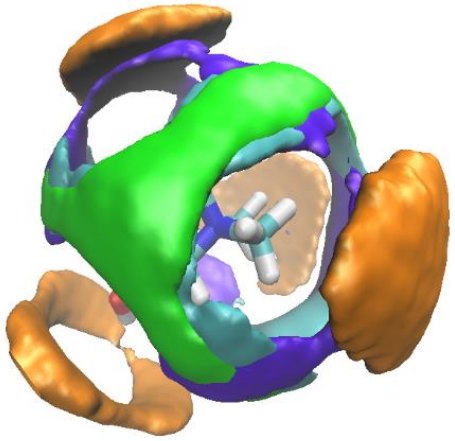

Figure 6. Spatial distribution functions of the chloride (green), water (cyan), hydroxyl (blue) and methyl (brown) group surrounding a reference choline's ammonium, as obtained from MD simulations of aquoline at 298 K (isovalue= 25% of maximum amplitude).

(green), water (cyan) and choline's hydroxyl (blue) groups around the choline's ammonium are shown. This Figure highlights the different distribution of polar moieties and hydrophobic methyl groups (brown). Anions, water and hydroxyl groups approach the ammonium as close as possible to the nitrogen atom that bears most of the cation positive charge. Accordingly they tend to distribute intercalating between neighbour methyl groups forming a characteristic distribution similar to the

one observed in the case of water solvation of tetramethylammonium cations,[31] leaving three holes facing to the N-methyl group axis. Such holes are occupied at larger distances by either methyl groups or other hydroxyl groups.

Figure 7 shows the spatial distribution functions of the same moieties around reference hydroxyl group in choline. While the anion (green) is directly facing the O–H bond (as confirmed by the narrow distribution of the O–H···Cl angle around linearity, data not shown), water (cyan) is distributed as capping the hydroxyl group, at a closer distance than chloride, due to the possibility to behave both as HB acceptor and donor. Hydroxyl (blue) and ammonium (mauve) groups from neighbour choline cations tend to distribute over a much wider location, solvating not only the

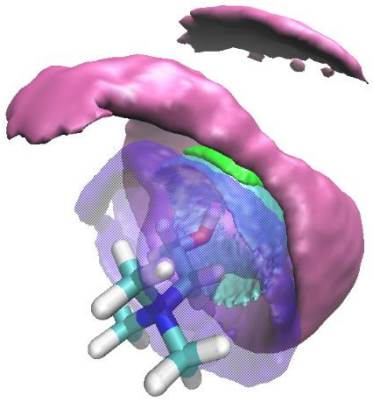

Figure 7. Spatial distribution functions of the chloride (green), water (cyan), hydroxyl (blue) and nitrogen (mauve) group surrounding a reference choline's hydroxyl group, as obtained from MD simulations of aquoline at 298 K (isovalue= 25% of maximum amplitude).

hydroxyl group but also its neighbour methylene moieties. Further inspection of SDF's referring to the second solvation shells to choline shows, in agreement with **Figures 3 and 4**, the presence of close anions and water moieties and, at even larger distances, surrounding shells of ammonium and hydroxyl moieties. At odd with the case of reline, where the anion is sandwiched by the cation and the HBD (urea), in the present case both anion and HBD (water) equally share their distribution locations around the cation's polar extremes. We also observe that choline location around the reference one occurs at much larger distance than the two other moieties (water and chloride) and it is rather homogeneously distributed, wrapping the reference choline.

We further extend our analysis on the choline's hydroxyl and ammonium solvation scenario; the PDF's and SDF's shown in **Figure 5 and 6-7**, respectively, reflect the complex environment

surrounding Och and Nch. In order to explore this complexity, we evaluated the combined distribution functions (CDF) build up by two PDFs, having as a reference either Och or Nch. A generic CDFs from this analysis e.g. the one obtained by g(r) Och-X and g(r) Och-Y (where X and Y are different moieties potentially solvating choline's oxygen) is a 3-D plot (represented as heat map) whose amplitude, point by point ([x,y]), is proportional to the *co-occurrence* of an atom X distant x Å from the reference Och *and* an atom Y distant y Å from the same reference Och. Hot lobes appearing in these plots highlight the existence of a coordinated solvation of the reference moiety (in our case Och) by the two entities, with a given coordination geometry. Accordingly, they would indicate the existence of a structural *leit-motif* characterising the environment surrounding the reference. In **Figure 8**, we show two CDF's referring to the joint coordination of a reference Och by the following couples of solvating moieties: a) [Ow,Ow] and b) [Ow, Cl] (other relevant, though of lower importance, coordination options are shown in **Figure S3** of the SI). These plots indicate that the most recurrent solvation mechanism involves two water molecules that can occupy three hot lobes, namely [2.9; 4.3], [4.3; 2.9] and [4.3; 4.3] (see **Figure 8 a)**). The second most recurrent solvation *leit-motif* is the one where simultaneous coordination by one water molecule and one chloride anion occurs, with a hot lobe at [Ow; Cl]=[4.2; 3.1] (see **Figure 8 b)**). Other solvation mechanisms (see **Figure S3** of the SI) do not look of comparable statistical relevance as the previous ones. The information extracted from **Figure 8** is highly complementary to the one contained in **Figure 5 and 6**. The latter Figures suggest that choline's hydroxyl group is surrounded mostly by water, chlorine anions and other choline oxygens, but inspection of **Figures 6 and S3** (in the SI) suggests that only water and chloride species can provide a statistically relevant coordination mechanism. Such a coordination scheme might resemble a clathrate-like structure, where water and chlorine form a cage surrounding the reference hydroxyl group.

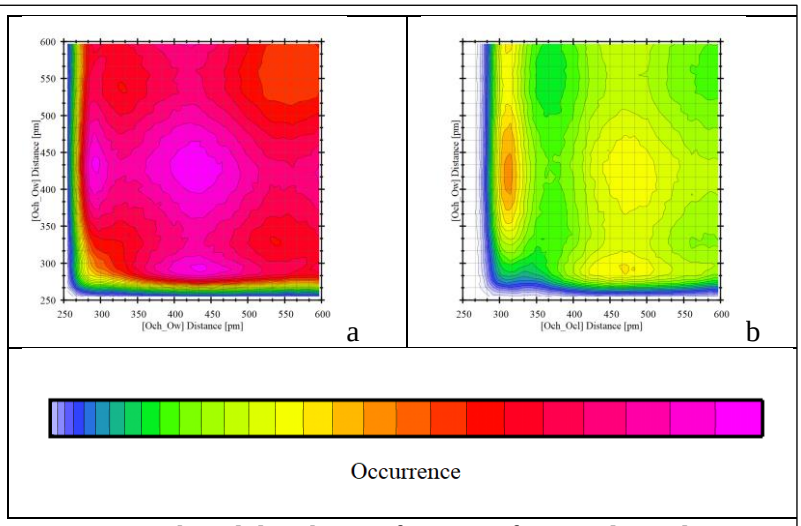

Figure 8. Combined distribution functions for coordinated correlation with reference Och by the following couples of solvating moieties: a) [Ow, Ow] and b) [Ow, Cl], as obtained from MD simulations of aquoline at 298 K.

Analogous analysis can be done with a reference Nch: the most relevant CDF plot (two water molecules coordinating the choline's nitrogen) is shown in **Figure 9** (other CDFs are shown in **Figures S4** of the ESI). Here the situation is different from the Och case. The limited access granted

by the methyl groups to the charged ammonium nitrogen determines well defined locations for close access to nitrogen. It emerges from **Figures 5 and 7** that close contacts between water, chloride or hydroxyl group and Nch are allowed only through an intrusion between the ammonium methyl groups. Accordingly, this leads to spots where the different coordinating species can locate without interfering too much with each other: the two closest entities to this choline extreme location are water molecules that can get simultaneously as close as 4.6 Å to the nitrogen atom (see **Figure 9**). The next couple that can favourably access the nitrogen atom involves water and chloride that can access at [4.6; 4.4] (see **Figure S4** in the SI). This and the other pairs (see **Figure S4** in the SI), do not show, however, a statistical relevance as compared to the water-water pair.

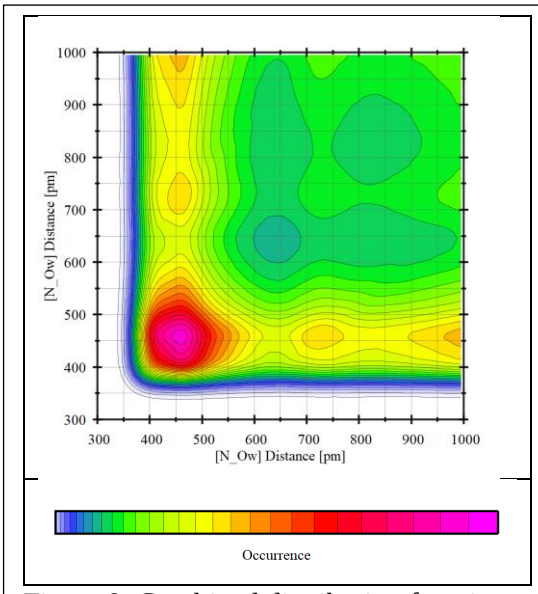

Figure 9. Combined distribution function for coordinated correlation of reference Nch by the [Ow, Ow] pair as obtained from MD simulations of aquoline at 298 K.

We also explored the nature of HB connectivity across the simulation box, between water and chloride moieties. In order to do that we used the ChemNetworks approach developed by Clark and coworkers.[52] By imposing geometrical conditions to HB definitions (namely for the O-H··O interaction, we defined the distance $d_{H\cdot\cdot O}$<2.5Å and the angle 150°<$\theta_{O\text{-}H\cdot\cdot O}$<180°, while for the O-H··Cl interaction, we defined the distance $d_{H\cdot\cdot Cl}$<2.6Å and the angle 150°<$\theta_{O\text{-}H\cdot\cdot Cl}$<180°), we monitored the length of the chains formed by water-water and water-chloride HB mediated interactions. As it clearly emerges from **Figure 10**, chains involving water-water and water-chloride HB connections extend over a quite large number of members (non negligible population can be detected up to 40 members) with a population maximum at ca. 25 members.

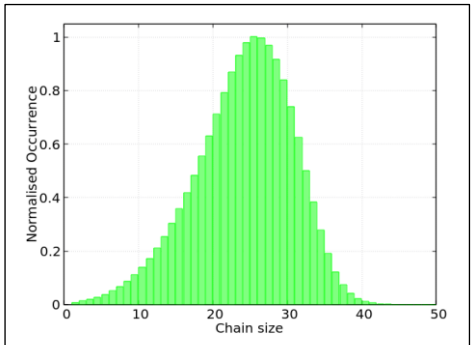

Figure 10. Distribution of the chains formed by hydrogen bonding mediated water-water + water-chlorine correlations, as obtained from MD simulations of aquoline at 298 K.

Conclusion.

We reported the first structural investigation of aquoline, a natural deep eutectic solvent (NADES) formed by choline chloride:water at ratio 1:3.33. Such a mixture, whose composition qualifies it as a water-in-salt compound, does not show crystallization events down to 183 K. Based on molecular dynamics computations, we extracted accurate structural information on aquoline at 298 K, in its liquid state. Computed X-ray and neutron scattering patterns reveal interesting features. We find that, upon selective deuteration of either water or of choline, a distinct low Q feature manifests between 0.9 and 1.1 $Å^{-1}$. In other related systems, such an occurrence fingerprints the existence of polar-apolar structural alternations that characterise the mesoscopic scale morphology. Although here we cannot properly individuate an apolar moiety, nevertheless a differentiation between a) choline and b) water and chloride can provide a rationalization to the observed behaviour in terms of an alternation between a) and b) moieties.

Our subsequent analysis leads to the observation that both water and chloride strongly compete with each other to coordinate the ammonium and the hydroxyl moieties in choline. In agreement with the proposal from Harmon et al.[65] on ChCl di-hydrate, despite being liquid (and actually a very fluid liquid, as compared to other ChCl-based DES), aquoline's cation environment turns out to be very structured. The solvation of choline hydroxyl moiety occurs through a synergistic competition between water/water or water/chloride moieties; the ammonium solvation is less competitive, although, due to the steric hindrance from methyl groups, the different moieties can access the charged nitrogen only at specific locations, intruding between the methyl groups. At larger spatial scales, choline is further solvated by other cations that develop a sort of sheath surrounding the water- and chloride- solvated reference choline. Due to their size and (partial) charges, water and chloride interact very strongly and at very short range. At odd with the behaviour of other DES, where the HBD organises with more than one solvation shell of similar molecules, in aquoline, water interacts with other water molecules only developing a short range first solvation shell: at larger distances a water depletion regime is detected. The interactions with chloride and choline moieties hinders the formation of a more bulk water-like environment around reference water. A network analysis shows that water and chlorine can engage HB-mediated interactions over a large spatial scale, with chains containing as many as 40 members and with a population maximum occurring at 25 members. Overall the structural scenario that we identify based on this information consists of strongly water and chloride solvated choline cations dispersed in the bulk phase and surrounded by other neighbour cations, with wires of water and chloride merging such objects.

This study provides the first exploration of water-in-salt NADES on the basis of computational tools. The emerging structural scenario prompts for further investigations based on X-ray and neutron scattering as well as other techniques (e.g. NMR and IR/Raman spectroscopy) to explore structural and dynamic features at different water content and temperature/pressure conditions. Such studies are currently under development and will be reported subsequently.

Conflicts of interest

There are no conflicts to declare.

Acknowledgements.

This work has been supported by the University of Rome Sapienza Projects: "Microscopic and mesoscopic organization in ionic liquid-based systems." (RG11715C7CC660BE) and “Green solvents for simple and complex carbohydrates” (RM120172B2165468).

M.B. acknowledges financial support by the Deutsche Forschungsgemeinschaft (DFG) through project Br 5494/1-1.

Access to S. Brutti’s laboratories (Univ. Rome – Sapienza) is gratefully acknowledged. Access to the SAXS-Lab at the University of Rome Sapienza and support from Dr. A. Del Giudice are acknowledged.

Bibliography.

1 Y. H. Choi, J. van Spronsen, Y. Dai, M. Verberne, F. Hollmann, I. W. C. E. Arends, G. J. Witkamp and R. Verpoorte, Are natural deep eutectic solvents the missing link in understanding cellular metabolism and physiology?, *Plant Physiol.*, 2011, **156**, 1701–1705.

2 Y. Dai, J. van Spronsen, G. J. Witkamp, R. Verpoorte and Y. H. Choi, Natural deep eutectic solvents as new potential media for green technology, *Anal. Chim. Acta*, 2013, **766**, 61–68.

3 Y. Dai, J. Van Spronsen, G. J. Witkamp, R. Verpoorte and Y. H. Choi, Ionic liquids and deep eutectic solvents in natural products research: Mixtures of solids as extraction solvents, *J. Nat. Prod.*, 2013, **76**, 2162–2173.

4 R. Craveiro, I. Aroso, V. Flammia, T. Carvalho, M. T. Viciosa, M. Dionísio, S. Barreiros, R. L. Reis, A. R. C. Duarte and A. Paiva, Properties and thermal behavior of natural deep eutectic solvents, *J. Mol. Liq.*, 2016, **215**, 534–540.

5 A. Paiva, R. Craveiro, I. Aroso, M. Martins, R. L. Reis and A. R. C. Duarte, Natural deep eutectic solvents - Solvents for the 21st century, *ACS Sustain. Chem. Eng.*, 2014, **2**, 1063–1071.

6 A. P. Abbott, G. Capper, D. L. Davies, R. K. Rasheed and V. Tambyrajah, Novel solvent properties of choline chloride/urea mixtures, *Chem. Commun.*, 2003, 70–71.

7 C. D. Agostino, R. C. Harris, A. P. Abbott, F. Gladden and M. D. Mantle, Molecular motion and ion diffusion in choline chloride based deep eutectic solvents studied by 1 H pulsed field gradient NMR spectroscopy, 2011, 21383–21391.

8 M. Gilmore, L. M. Moura, A. H. Turner, M. Swadźba-Kwaśny, S. K. Callear, J. A. McCune, O. A. Scherman and J. D. Holbrey, A comparison of choline:urea and choline:oxalic acid deep eutectic solvents at 338 K, *J. Chem. Phys.*, , DOI:10.1063/1.5010246.

9 M. Gilmore, M. Swadzba-Kwasny and J. D. Holbrey, Thermal Properties of Choline Chloride/Urea System Studied under Moisture-Free Atmosphere, *J. Chem. Eng. Data*, 2019, **64**, 5248–5255.

10 E. L. Smith, A. P. Abbott and K. S. Ryder, Deep Eutectic Solvents (DESs) and Their Applications, *Chem. Rev.*, 2014, **114**, 11060–11082.

11 O. S. Hammond, D. T. Bowron and K. J. Edler, Liquid structure of the choline chloride-urea deep eutectic solvent (reline) from neutron diffraction and atomistic modelling, *Green*

Chem., 2016, **18**, 2736–2744.

12 A. P. Abbott, P. M. Cullis, M. J. Gibson, R. C. Harris and E. Raven, Extraction of glycerol from biodiesel into a eutectic based ionic liquid, 2007, 868–872.

13 Z. Maugeri and P. Domínguez De María, Novel choline-chloride-based deep-eutectic-solvents with renewable hydrogen bond donors: Levulinic acid and sugar-based polyols, *RSC Adv.*, 2012, **2**, 421–425.

14 A. H. Turner and J. D. Holbrey, Supporting Information : Investigation of glycerol hydrogen-bonding networks in choline chloride / glycerol eutectic-forming liquids using neutron diffraction, 2019, 1–5.

15 O. S. Hammond, D. T. Bowron, A. J. Jackson, T. Arnold, A. Sanchez-Fernandez, N. Tsapatsaris, V. Garcia Sakai and K. J. Edler, Resilience of Malic Acid Natural Deep Eutectic Solvent Nanostructure to Solidification and Hydration, *J. Phys. Chem. B*, 2017, **121**, 7473–7483.

16 O. S. Hammond, D. T. Bowron and K. J. Edler, The Effect of Water upon Deep Eutectic Solvent Nanostructure: An Unusual Transition from Ionic Mixture to Aqueous Solution, *Angew. Chemie - Int. Ed.*, 2017, **56**, 9782–9785.

17 R. Stefanovic, M. Ludwig, G. B. Webber, R. Atkin and A. J. Page, Nanostructure, hydrogen bonding and rheology in choline chloride deep eutectic solvents as a function of the hydrogen bond donor, *Phys. Chem. Chem. Phys.*, 2017, **19**, 3297–3306.

18 L. C. Brown, J. M. Hogg, M. Gilmore, L. Moura, S. Imberti, S. Gärtner, H. Q. N. Gunaratne, R. J. O'Donnell, N. Artioli, J. D. Holbrey and M. Swadźba-Kwaśny, Frustrated Lewis pairs in ionic liquids and molecular solvents-a neutron scattering and NMR study of encounter complexes, *Chem. Commun.*, 2018, **54**, 8689–8692.

19 P. Kumari, Shobhna, S. Kaur and H. K. Kashyap, Influence of Hydration on the Structure of Reline Deep Eutectic Solvent: A Molecular Dynamics Study, *ACS Omega*, 2018, **3**, 15246–15255.

20 E. O. Fetisov, D. B. Harwood, I. F. W. Kuo, S. E. E. Warrag, M. C. Kroon, C. J. Peters and J. I. Siepmann, First-Principles Molecular Dynamics Study of a Deep Eutectic Solvent: Choline Chloride/Urea and Its Mixture with Water, *J. Phys. Chem. B*, 2018, **122**, 1245–1254.

21 H. Zhang, M. L. Ferrer, M. J. Roldán-Ruiz, R. J. Jiménez-Riobóo, M. C. Gutiérrez and F.

Del Monte, Brillouin Spectroscopy as a Suitable Technique for the Determination of the Eutectic Composition in Mixtures of Choline Chloride and Water, *J. Phys. Chem. B*, 2020, **124**, 4002–4009.

22 M. S. Rahman and D. E. Raynie, Thermal behavior, solvatochromic parameters, and metal halide solvation of the novel water-based deep eutectic solvents, *J. Mol. Liq.*, 2020, **3**, 114779.

23 Y. Marcus, Unconventional Deep Eutectic Solvents: Aqueous Salt Hydrates, *ACS Sustain. Chem. Eng.*, 2017, **5**, 11780–11787.

24 L. Suo, O. Borodin, T. Gao, M. Olguin, J. Ho, X. Fan, C. Luo, C. Wang and K. Xu, 'Water-in-salt' electrolyte enables high-voltage aqueous lithium-ion chemistries, *Science (80-.).*, 2015, **350**, 938–943.

25 L. Suo, O. Borodin, W. Sun, X. Fan, C. Yang, F. Wang, T. Gao, Z. Ma, M. Schroeder, A. von Cresce, S. M. Russell, M. Armand, A. Angell, K. Xu and C. Wang, Advanced High-Voltage Aqueous Lithium-Ion Battery Enabled by "Water-in-Bisalt" Electrolyte, *Angew. Chemie - Int. Ed.*, 2016, **55**, 7136–7141.

26 Y. Yamada, K. Usui, K. Sodeyama, S. Ko, Y. Tateyama and A. Yamada, Hydrate-melt electrolytes for high-energy-density aqueous batteries, *Nat. Energy*, 2016, **1**, 16129.

27 B. Safe, L. Suo, O. Borodin, Y. Wang, X. Rong, W. Sun, X. Fan, S. Xu, M. A. Schroeder, A. V Cresce, F. Wang, C. Yang, Y. Hu, K. Xu and C. Wang, "Water-in-Salt" Electrolyte Makes Aqueous Sodium-Ion Battery Safe, Green, and Long-Lasting, *Adv. Energy Mater.*, 2017, 1701189.

28 V. Agieienko and R. Buchner, Densities, Viscosities, and Electrical Conductivities of Pure Anhydrous Reline and Its Mixtures with Water in the Temperature Range (293.15 to 338.15) K, *J. Chem. Eng. Data*, 2019, **64**, 4763–4774.

29 A. R. Harifi-Mood and R. Buchner, Density, viscosity, and conductivity of choline chloride + ethylene glycol as a deep eutectic solvent and its binary mixtures with dimethyl sulfoxide, *J. Mol. Liq.*, 2017, **225**, 689–695.

30 K. M. Harmon and G. F. Avci, Hydrogen bonding. Part 17. IR and NMR study of the lower hydrates of choline chloride, *J. Mol. Struct.*, 1984, **118**, 267–275.

31 E. J. Nilsson, V. Alfredsson, D. T. Bowron and K. J. Edler, A neutron scattering and

modelling study of aqueous solutions of tetramethylammonium and tetrapropylammonium bromide, *Phys. Chem. Chem. Phys.*, 2016, **18**, 11193–11201.

32 T. I. Morrow and E. J. Maginn, Density, local composition and diffusivity of aqueous choline chloride solutions: A molecular dynamics study, *Fluid Phase Equilib.*, 2004, **217**, 97–104.

33 S. Shaukat, M. V. Fedotova, S. E. Kruchinin, M. Bešter-Rogač, Č. Podlipnik and R. Buchner, Hydration and ion association of aqueous choline chloride and chlorocholine chloride, *Phys. Chem. Chem. Phys.*, 2019, **21**, 10970–10980.

34 S. M. Vilas-Boas, D. O. Abranches, E. A. Crespo, O. Ferreira, J. A. P. Coutinho and S. P. Pinho, Experimental solubility and density studies on aqueous solutions of quaternary ammonium halides, and thermodynamic modelling for melting enthalpy estimations, *J. Mol. Liq.*, , DOI:10.1016/j.molliq.2019.112281.

35 B. Hess, C. Kutzner, D. Van Der Spoel and E. Lindahl, GRGMACS 4: Algorithms for highly efficient, load-balanced, and scalable molecular simulation, *J. Chem. Theory Comput.*, 2008, **4**, 435–447.

36 D. Van Der Spoel, E. Lindahl, B. Hess, G. Groenhof, A. E. Mark and H. J. C. Berendsen, GROMACS: Fast, flexible, and free, *J. Comput. Chem.*, 2005, **26**, 1701–1718.

37 B. Doherty and O. Acevedo, OPLS Force Field for Choline Chloride-Based Deep Eutectic Solvents, *J. Phys. Chem. B*, 2018, **122**, 9982–9993.

38 W. L. Jorgensen, J. Chandrasekhar, J. D. Madura, R. W. Impey and M. L. Klein, Comparison of simple potential functions for simulating liquid water, *J. Chem. Phys.*, 1983, **79**, 926–935.

39 L. Martínez, R. Andrade, E. G. Birgin and J. M. Martínez, PACKMOL: A package for building initial configurations for molecular dynamics simulations, *J. Comput. Chem.*, 2009, **30**, 2157–2164.

40 H. J. C. Berendsen, J. P. M. Postma, W. F. Van Gunsteren, A. Dinola and J. R. Haak, Molecular dynamics with coupling to an external bath, *J. Chem. Phys.*, 1984, **81**, 3684–3690.

41 G. Bussi, D. Donadio and M. Parrinello, Canonical sampling through velocity rescaling, *J. Chem. Phys.*, 2007, **126**, 014101.

42 M. Parrinello and A. Rahman, Polymorphic transitions in single crystals: A new molecular dynamics method, *J. Appl. Phys.*, 1981, **52**, 7182–7190.

43 T. Darden, D. York and L. Pedersen, Particle mesh Ewald: An N·log(N) method for Ewald

sums in large systems, *J. Chem. Phys.*, 1993, **98**, 10089–10092.

44 U. Essmann, L. Perera, M. L. Berkowitz, T. Darden, H. Lee and L. G. Pedersen, A smooth particle mesh Ewald method, *J. Chem. Phys.*, 1995, **103**, 8577–8593.

45 M. Brehm and B. Kirchner, TRAVIS - A free analyzer and visualizer for monte carlo and molecular dynamics trajectories, *J. Chem. Inf. Model.*, 2011, **51**, 2007–2023.

46 O. Hollóczki, M. Macchiagodena, H. Weber, M. Thomas, M. Brehm, A. Stark, O. Russina, A. Triolo and B. Kirchner, Triphilic Ionic-Liquid Mixtures: Fluorinated and Non-fluorinated Aprotic Ionic-Liquid Mixtures, *ChemPhysChem*, 2015, **16**, 3325–3333.

47 M. Brehm, M. Thomas, S. Gehrke and B. Kirchner, TRAVIS—A free analyzer for trajectories from molecular simulation, *J. Chem. Phys.*, 2020, **152**, 164105.

48 F. Lo Celso, Y. Yoshida, F. Castiglione, M. Ferro, A. Mele, C. J. Jafta, A. Triolo and O. Russina, Direct experimental observation of mesoscopic fluorous domains in fluorinated room temperature ionic liquids, *Phys. Chem. Chem. Phys.*, 2017, **19**, 13101–13110.

49 F. Lo Celso, G. B. Appetecchi, C. J. Jafta, L. Gontrani, J. N. Canongia Lopes, A. Triolo and O. Russina, Nanoscale organization in the fluorinated room temperature ionic liquid: Tetraethyl ammonium (trifluoromethanesulfonyl)(nonafluorobutylsulfonyl)imide, *J. Chem. Phys.*, , DOI:10.1063/1.5016236.

50 F. Lo Celso, G. B. Appetecchi, E. Simonetti, M. Zhao, E. W. Castner, U. Keiderling, L. Gontrani, A. Triolo and O. Russina, Microscopic Structural and Dynamic Features in Triphilic Room Temperature Ionic Liquids, *Front. Chem.*, 2019, **7**, 1–14.

51 F. Lo Celso, G. B. Appetecchi, E. Simonetti, U. Keiderling, L. Gontrani, A. Triolo and O. Russina, Mesoscopic structural organization in fluorinated pyrrolidinium-based room temperature ionic liquids, *J. Mol. Liq.*, 2019, **289**, 111110.

52 A. Ozkanlar and A. E. Clark, ChemNetworks: A complex network analysis tool for chemical systems, *J. Comput. Chem.*, 2014, **35**, 495–505.

53 I. M. Hodge, Enthalpy relaxation and recovery in amorphous materials, *J. Non. Cryst. Solids*, 1994, **169**, 211–266.

54 H. V. R. Annapureddy, H. K. Kashyap, P. M. De Biase and C. J. Margulis, What is the origin of the prepeak in the x-ray scattering of imidazolium-based room-temperature ionic liquids?, *J. Phys. Chem. B*, 2010, **114**, 16838–16846.

55 H. K. Kashyap, J. J. Hettige, H. V. R. Annapureddy and C. J. Margulis, SI - SAXS anti-peaks reveal the length-scales of dual positive-negative and polar-apolar ordering in room-temperature ionic liquids., *Chem. Commun.*, 2012, **48**, 5103–5.

56 J. C. Araque, J. J. Hettige and C. J. Margulis, Modern Room Temperature Ionic Liquids, a Simple Guide to Understanding Their Structure and How It May Relate to Dynamics, *J. Phys. Chem. B*, 2015, **119**, 12727–12740.

57 S. Kaur, S. Sharma, H. K. Kashyap, S. Kaur, S. Sharma and H. K. Kashyap, Bulk and interfacial structures of reline deep eutectic solvent : A molecular dynamics study Bulk and interfacial structures of reline deep eutectic solvent : A molecular dynamics study, *J. Chem. Phys.*, 2017, **147**, 194507.

58 S. Kaur, A. Malik and H. K. Kashyap, Anatomy of Microscopic Structure of Ethaline Deep Eutectic Solvent Decoded through Molecular Dynamics Simulations, *J. Phys. Chem. B*, 2019, **123**, 8291–8299.

59 A. Triolo, F. Lo Celso, C. Ottaviani, P. Ji, G. B. Appetecchi, F. Leonelli, D. S. Keeble and O. Russina, Structural features of selected protic ionic liquids based on a super-strong base, *Phys. Chem. Chem. Phys.*, 2019, **21**, 25369–25378.

60 H. K. Kashyap, J. J. Hettige, H. V. R. Annapureddy and C. J. Margulis, SAXS anti-peaks reveal the length-scales of dual positive–negative and polar–apolar ordering in room-temperature ionic liquids, *Chem. Commun.*, 2012, **48**, 5103.

61 J. J. Hettige, J. C. Araque and C. J. Margulis, Bicontinuity and multiple length scale ordering in triphilic hydrogen-bonding ionic liquids, *J. Phys. Chem. B*, 2014, **118**, 12706–12716.

62 O. S. Hammond, D. T. Bowron, A. J. Jackson, T. Arnold, A. Sanchez-fernandez, N. Tsapatsaris, V. G. Sakai and K. J. Edler, Resilience of Malic Acid Natural Deep Eutectic Solvent Nanostructure to Solidi fi cation and Hydration, , DOI:10.1021/acs.jpcb.7b05454.

63 A. K. Soper and C. J. Benmore, Quantum Differences between Heavy and Light Water, *Phys. Rev. Lett.*, 2008, **101**, 065502.

64 S. Zahn, Deep eutectic solvents: similia similibus solvuntur?, *Phys. Chem. Chem. Phys.*, 2017, **19**, 4041–4047.

65 K. M. Harmon, A. C. Akin, G. F. Avci, L. S. Nowos and M. B. Tierney, Hydrogen bonding. Part 33. NMR study of the hydration of choline and acetylcholine halides, *J. Mol. Struct.*,

1991, **244**, 223–236.